Planar Helium under Electromagnetic Driving

Javier Madroñero and Andreas Buchleitner

Max-Planck-Institut für Physik komplexer Systeme,
Nöthnitzer Str. 38, D-01187 Dresden
jma@mpipks-dresden.mpg.de, abu@mpipks-dresden.mpg.de

We report on the successful numerical implementation of an original method for the accurate quantum treatment of helium under electromagnetic driving. Our approach is the first to allow for a description of the highly complex quantum dynamics of this system, in the entire non-relativistic parameter regime, i.e., it provides full spectral and dynamical information on the ionization of the atomic ground state by optical fields, as well as on the dynamics of doubly excited Rydberg states under radiofrequency driving. As a by-product, the non-trivial role of the dimension of configuration space for the field-free dynamics of doubly excited helium is elucidated.

1 Introduction

The quantum mechanical treatment of the helium atom goes back to the early days of quantum mechanics: Einstein was the first [1] to realize that the then available quantization schemes which had been applied successfully in the analysis of the atomic spectra of one electron atoms would be inoperational for this microscopic realization of the gravitational three body problem: As first noticed by Poincaré, the classical dynamics of the latter is nonintegrable, and this remains true when gravitational forces are substituted by attractive and repulsive Coulomb forces, such as to define the three body Coulomb problem. Indeed, the electron-electron interaction term in the Hamiltonian of the unperturbed helium atom – which otherwise is just the sum of two hydrogen Hamiltonians with amended nuclear charge – renders the two-electron dynamics in general irregular or chaotic, with only rather small domains of the classical phase space occupied by regular, i.e., integrable, motion. On the quantum level, the loss of integrability is tantamount to the (at least partial) destruction of good quantum numbers, and leads to an abundance of intriguing and surprising effects, such as the autoionization of doubly excited states [2], Ericson fluctuations in the photocrossection at high excitation energies [3], and highly asymmetric though very stable frozen planet configurations of the

doubly excited atom [4, 5]. Hence, even without any external perturbation, doubly excited states of helium represent one of the most challenging – and experimentally accessible [6] – test cases for the theory of quantum chaos [7], which deals with low dimensional, complex though completely deterministic (in the sense of the absence of any random forcing) quantum dynamics.

However, after hydrogen, helium is also the simplest naturally available atomic species, and therefore a natural candidate for the investigation of light-matter interaction. As compared to one electron atoms, it precisely adds the additional electron-electron interaction term, which is a source of electronic correlations. Since the interaction of atoms with coherent radiation defines a quantum transport problem along the energy axis (the atomic electron(s) extract and/or reemit energy from/into the driving field), helium allows for the systematic experimental and theoretical study of the influence of electronic correlation on quantum transport. With recent progress in the experimental characterization of the light-induced fragmentation process in the presence of electronic correlations [8, 9], an accurate theoretical treatment becomes ever more desirable. The latter, however, defines a formidable theoretical and numerical challenge: Under linearly polarized driving only the projection of the total angular momentum onto the polarization axis, together with a generalized parity which encompasses the phase of the driving field, remains a conserved quantity – all the other good quantum numbers are mixed by the external perturbation. Consequently, the density of states dramatically increases with the excitation of the electrons as well as with the order of the multiphoton excitation process induced by the external field. Therefore, a fully three dimensional treatment of the driven helium problem for arbitrary driving frequencies and electronic excitations still remains beyond reach of the largest supercomputers currently available, simply due to the rapidly increasing size of Hilbert space as more and more angular momenta are coupled by the field. Note, however, that three dimensional ab initio treatments [10, 11, 12, 13] of the ionization of helium from the atomic ground state are available, though cannot resolve the transient population of highly excited states in the course of the ionization process. Neither has it been demonstrated so far that they bear the potential to describe the dynamics of highly excited initial states under electromagnetic driving.

Our own approach is different, and aims at the full spectral information underlying the atomic excitation and ionization process in the presence of electronic correlations, for arbitrary atomic initial states, and arbitrary driving field frequencies and intensities (within the nonrelativistic regime). It combines the representation of the atomic Hamiltonian in a suitably chosen basis set, which allows for fully algebraic expressions of the matrix elements (employing symbolic calculus), the Floquet theorem [14] to account for the periodicity of the external perturbation, and complex dilation [15] such as to access the atomic decay rates (due to autoionization and/or induced by the external field) [16]. Complex dilation being a non-unitary similarity transformation of the Floquet Hamiltonian finally leaves us with a large, generalized,

complex symmetric eigenvalue problem, which has to be diagonalized on the most powerful parallel machines currently available. In order to gain insight into the dynamics of relevant observables in some predefined energy range, we need to extract only a (relatively, as compared to the total dimension of the basis) small number of complex eigenvalues, what is achieved with an efficient parallel implementation of the Lanczos diagonalization routine. Finally, parallel coding is also mandatory for the visualization of the dynamics of the atomic eigenstates in the field, given their rather large dimension and the quite intricate coordinate transformation leading to the above-mentioned algebraic treatment of the problem.

Note that the speed-up of program execution as one of the prominent advantages of a large parallel machine is vital for our project, since it accelerates our progresses tremendously. However, the availability of large storage space for the matrix to be diagonalized is a conditio sine qua non.

Yet, due to the above-mentioned rapid increase of the Hilbert space dimension (and hence, on the numerical level, of the required storage capacities), we still restrict our problem to planar configurations of the two electrons and the nucleus, with the field polarization axis within this plane. Whilst this certainly does restrict the generality of our model, semiclassical scaling arguments suggest that the unperturbed three body dynamics is essentially planar at high electronic excitations and small to moderate total angular momenta, and equally so highly correlated fragmentation processes starting from the atomic ground state [17, 18, 19]. Furthermore, the planar three body Coulomb problem has independent realizations in quasi two dimensional semiconductor structures [20], as well as in 2d quantum dots [21].

2 Theory

Let us start with the Hamiltonian describing our problem, in atomic units (which will be used throughout this paper),

$$H = \frac{p_1^2 + p_2^2}{2} - \frac{2}{r_1} - \frac{2}{r_2} + \frac{1}{r_{12}} + F(x_1 + x_2)\cos(\omega t) \ , \tag{1}$$

where p_i and r_i, $i = 1, 2$, design the respective momenta and positions of both electrons, r_{12} represents the interelectronic distance, the nucleus (with infinite mass) is fixed at the origin, and the field is polarized along the x-axis. Two subsequent, parabolic coordinate transformations, interleaved with a suitable rotation, completely regularize all singularities in this Hamiltonian and finally allow to identify the eigenvalue problem generated by (1) with an eigenvalue problem describing *four* coupled harmonic oscillators [17, 22]. Consequently, (1) can be represented in a basis set defined by the tensor product

$$|n_1 n_2 n_3 n_4\rangle = |n_1\rangle \otimes |n_2\rangle \otimes |n_3\rangle \otimes |n_4\rangle \tag{2}$$

of Fock states of the individual harmonic oscillators, and has a purely algebraic representation in the associated annihilation and creation operators that define the four oscillator algebras. The final eigenvalue problem involves polynomials of maximal degree 16 in the creation and annihilation operators, with alltogether 5472 monomial terms (generated by a home made Mathematica code [17]), and thus allows for a purely analytical calculation of all matrix elements defining our eigenvalue problem [17]. The final, complex symmetric matrix which we have to diagonalize is sparse banded, with 488 coupling matrix elements in the band. To minimize storage requirements, a separate (propagation) code [23] is used to determine the basis ordering which minimizes the band width of the matrix.

In a typical production run, for doubly excited helium with the inner electron's quantum number $N \simeq 6$, exposed to an electromagnetic field of frequency $\omega/2\pi \simeq 7895.55$ GHz (near resonant with the classical eigenfrequency of the frozen planet orbit which we will focus on below), the matrix dimension reaches values of $3\times10^5 \ldots 5.2\times10^5$, with a bandwidth of $2.6\times10^4 \ldots 4.6\times10^4$. This corresponds to storage requirements between 130 GB and 400 GB. The smaller ones of these eigenvalue problems are currently executed on the HITACHI SR8000-F1 at LRZ [24], whilst the larger ones are diagonalized on the IBM-Regatta at RZG [25]. Our parallel Lanczos code, which is composed of a Cholesky decomposition of the Hamiltonian matrix and a Lanczos iteration [26], performs very well on both machines, with typical monoprocessor performances of approx. 200–300 MFlops on the HITACHI and 600–1800 MFlops on the IBM. For very large matrix dimensions ($\simeq$ 200–300 GB), the monoprocessor performance is slightly improved using COMPAS on the HITACHI. On both machines, the code scales excellently [26] with the number of processors (which varies between 80 and 250 on the HITACHI, and between 32 and 512 on the IBM).

3 Results

In the following, we present some of our recent results, on the field-free as well as on the periodically driven frozen planet configuration of 2D helium. This configuration, which is a *dynamically stable* configuration of the unperturbed three-body Coulomb problem, is characterized by a near-collinear arrangement of nucleus and electron, with both electrons on the *same* side of the nucleus [4]. This highly asymmetric structure might appear counterintuitive on the first glance, though can be understood once one realizes the underlying dynamical process which stabilizes the configuration: the outer electron creates a static field that polarizes the inner electron, such that the latter is essentially localized along an extremal parabolic orbit familiar from the quantum treatment of hydrogen in a static electric field [27]. The fast oscillation of the inner electron along this highly eccentric orbit, in combination with the interelectronic repulsion, creates an effective potential minimum for the outer

electron (upon temporal average over the inner electron's motion), where the latter is consequently localized.

Indeed, the existence of these configurations has been proven by accurate 3D [4] and 1D [28] quantum calculations, and its discovery was even triggered by earlier laboratory experiments [27]. A surprising observation of the 1D calculations was, however, that the frozen planet, when restricted to one single dimension of configuration space, exhibits autoionization rates which are several orders of magnitude *smaller* than those of the real 3D atom. This contrasts a wide spread argument [29], according to which 1D models should exhibit enhanced autoionization rates as compared to the actual 3D problem, since in the 1D case no space is left for the electrons to avoid the detrimental Coulomb singularity of the electron-electron interaction term in (1). On the basis of simulations of the 3D classical dynamics the authors of the 1D calculation [28] therefore conjectured that, once again, the origin of this counterintuitive effect is caused by the dynamical stabilization mechanism sketched above: only not too large transverse deviations from the ideal collinear case maintain the stability – the region of classical stability has a finite extension in the phase space component spanned by the transverse dimension.

If this argument holds true, already the frozen planet configurations of planar helium should exhibit enhanced autoionization rates as compared to the 1D case, and this can be easily tested in our theoretical/numerical setup briefly sketched above. Table 1 compares the autoionization rates of 1D [28], 2D and 3D [30] collinear frozen planet states, with the 2D results obtained from a diagonalization of (1), with $F = 0$, in the doubly exicted energy range around $N \simeq 3 \ldots 10$.

Table 1. Decay rates of the frozen planet states of the 1D, 2D and 3D helium atom, in atomic units

N	1D	3D		2D	
		Singlet	Triplet	Singlet	Triplet
3	1.4×10^{-12}	1.1×10^{-5}	6.8×10^{-6}	3.4×10^{-6}	1.5×10^{-6}
4	4.4×10^{-12}	1.2×10^{-5}	4.4×10^{-6}	8.8×10^{-7}	4.2×10^{-7}
5	2.5×10^{-12}	2.0×10^{-6}	1.8×10^{-7}	3.7×10^{-6}	2.1×10^{-8}
6	1.0×10^{-13}	5.6×10^{-7}	3.3×10^{-8}	1.0×10^{-5}	5.6×10^{-9}
7	3.9×10^{-13}	2.0×10^{-7}	3.8×10^{-7}	1.3×10^{-7}	1.3×10^{-7}
8	1.5×10^{-13}	3.7×10^{-7}	1.4×10^{-7}	5.3×10^{-7}	3.2×10^{-7}
9	6.4×10^{-14}	1.2×10^{-6}	2.2×10^{-8}	1.6×10^{-7}	3.9×10^{-8}
10	2.8×10^{-14}	5.3×10^{-7}	3.5×10^{-8}	8.7×10^{-8}	3.7×10^{-8}

Clearly, the 2D rates are of the same order of magnitude as the 3D rates, and considerably larger than the 1D results. The unsystematic fluctuations of the 2D/3D differences are possibly due to chaos assisted tunneling [31], a trace which we will have to follow up in the future. However, the present results

already confirm the above picture gained from classical calculations, and imply an important caveat for oversimplified 1D models [29] of correlated electronic systems in 3D, where dynamical (and, in fact, often nonlinear) stabilization effects are easily underestimated. Fig. 1 finally shows the electronic density of the inner and of the outer electron of the planar frozen planet state for $N = 6$, with the inner electron apparently (note the parabolic nodal lines) localized along a highly eccentric Kepler ellipse, and the outer electron standing still in space.

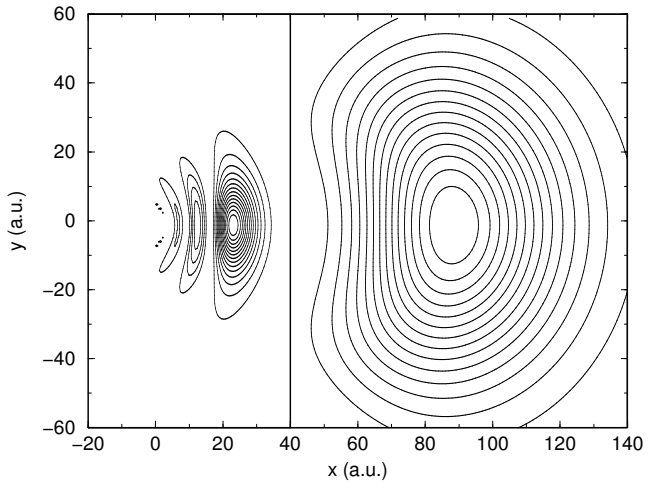

Fig. 1. Contour plot of the electronic density of the planar frozen planet state of the $N = 6$ series, in 2D configuration space. Whilst the inner electron (left) is localized along a highly eccentric Kepler ellipse (the nucleus sits in the origin), the outer electron (right) is "frozen" at the minimum of the effective potential dynamically created by the interplay between the electron-electron interaction term in (1) and the rapid Kepler motion of the inner electron along its strongly polarized trajectory [4, 27]

Apart from its independent interest for the field free, autonomous helium problem, the frozen planet configuration is of potentially high relevance in the context of coherent control [32] in the electronic dynamics of Rydberg systems in the presence of electron-electron interactions [33]: During the last decade, it has been realized that near-resonant electromagnetic driving of atomic electrons in one-electron Rydberg systems allows to create *nondispersive electronic wave packets* [34, 35, 36, 37] (in a quantum system with a *non-harmonic* spectrum!) which propagate along Kepler trajectories of essentially arbitrary eccentricity and orientation for very long times [34, 35, 38]. This field has by now been investigated theoretically in much detail and is

well understood, and first experimental realizations of such long living "quantum particles" have been reported very recently [39]. An immediate question is of course whether such a localization and stabilization effect is also to be expected in Rydberg systems with additional electron-electron interaction, e.g., in helium. Since the unperturbed frozen planet configuration has a well defined associated eigenfrequency, the external field can be tuned such as to drive that frequency near resonantly, and, as a matter of fact, it already was shown that nondispersive two-electron wave packets which propagate along the frozen planet trajetory *do exist* in the one dimensional model of helium mentioned above [28]. However, no verification of this result was so far available for 2D or 3D helium, simply due to the mere size of the corresponding Floquet eigenvalue problem, brought about by the field induced coupling of many angular momentum states. On the other hand we have already seen, in our discussion of the autoionization rates of the field free frozen planet, that the dimension of the accessible configuration space can be crucial in this system. Indeed, classical 3D simulations [40] of the near resonantly driven frozen planet dynamics suggest that the elliptic fixed point of the 1D classical dynamics – which gives rise to the existence of the nondispersive two-electron wave packet in the 1D quantum calculation – turns into an unstable fixed point in higher dimensions. Only an additional static field allows to stabilize this classical, driven frozen planet trajectory against rapid decorrelation and subsequent autoionization [28, 40]. Hence, a quantum calculation in 2D or 3D is clearly needed to clarify the issue.

Our present approach is precisely suited to provide the desired answer – as the first quantum treatment of a realistic model of driven helium in the doubly excited energy range. On the basis of semiclassical estimates and earlier 1D calculations, we recently could identify, for the first time, a two-electron wave packet in the highly intricate Floquet spectrum (see Fig. 2) of doubly excited 2D helium under external driving. Fig. 3 shows the electronic density of the outer electron projected on the classical phase space component spanned by x_1 and p_1 [17, 28], with the inner electron fixed at $x_2 \simeq 0$, for different phases of the driving field. For comparison, also the classical phase space structure of the restricted collinear dynamics is shown. Clearly, the electronic wave function propagates along the collinear frozen planet trajectory, without dispersion! So far, we could not detect any indication of the classically observed transverse instability mentioned above, apart from the relatively large ionization rate $\Gamma = 8.7 \times 10^{-6}$ a.u., which differs from the 1D rate by approx. the same factor as observed in the above comparison (see table 1) of the autoionzation rates of the field free frozen planet states in different dimensions. This strong transverse localization of the quantum eigenstate of the driven 2D system as compared to the classical dynamics can have various causes, such as dynamical or semiclassical localization [41], but remains to be elucidated. Understanding its origin is of primordial importance, if only for a robust estimation of the scaling of the two-electron wave packet's ionization rate with the excitation energy determined by the inner electron's quantum number N: Our present

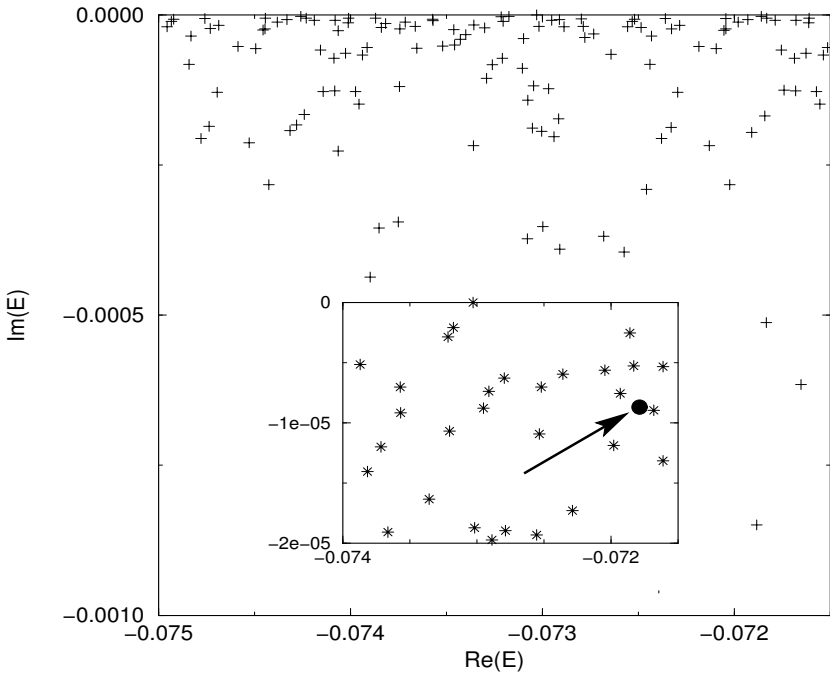

Fig. 2. Complex Floquet spectrum of the Floquet Hamiltonian derived [14] from (1), in the lower half of the complex plane. The real parts of the resonance poles (crosses or stars) correspond to the energies, the imaginary parts to half the decay rates of the atomic resonance states in the field [16]. The inset zooms into the vicinity of the wave packet eigenstate of Fig. 3, which is highlighted by a black spot and an arrow. $F = 12.8 \times 10^3$ V/cm, $\omega/2\pi = 7895.55$ GHz

example, which exhausts more than half the storage capacity of the IBM Regatta, but already nicely illustrates the desired, time-periodic localization properties of the wave packet, has been obtained for $N = 6$ (still quite some distance from the semiclassical limit of quasi-classical motion) and therefore is not yet expected to provide extremely long lived atomic eigenstates in the field [38]. Whilst the presently calculated life time $\Gamma^{-1} \simeq 21.9 \times 2\pi/\omega$ is already satisfactory for standard wave packets [42], it is nontheless still far from the life times expected for nondispersive wave packets in one electron Rydberg systems [38]. Though, from the point of view of coherent control, it is precisely the long life time which makes these objects so interesting (they allow the "storage" of electronic density at essentially arbitrary locations of phase space), and this is therefore one of the major routes of research which we wish to follow in the future.

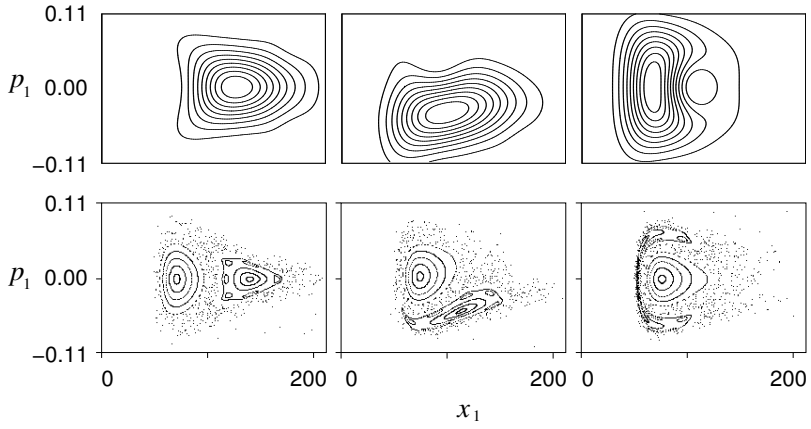

Fig. 3. Contour plot of the electronic density (top) of the wave packet eigenstate along the $N = 6$ frozen planet trajectory of 2D helium, under electromagnetic driving at frequency $\omega/2\pi = 7895.55$ GHz and amplitude $F = 12.8 \times 10^3$ V/cm, projected (as a quasiprobability Husimi distribution [28], for the inner electron's position fixed at $x_2 \simeq 0$) onto the phase space component spanned by x_1 and p_1, the position and momentum of the outer electron. For comparison, also the classical phase space structure of the restricted collinear problem [40] is shown (bottom), for the same values of the driving field's phase, $\omega t = 0, \pi/2, \pi$, from left to right. Clearly, the electron follows the classical frozen planet dynamics, without dispersion

It is a pleasure to thank Peter Schlagheck, Laurent Hilico, Benoît Grémaud, and Dominique Delande for lots of illuminating discussions and insight, and the HLRB team for excellent support, service and advice during the entire period of this project.

References

1. Einstein A.: Verh. Dtsch. Phys. Ges. **19**, 82 (1917).
2. Domke M., Schulz K., Remmers G., Kaindl G., and Wintgen D.: Phys. Rev. A **53**, 1424 (1996).
3. Grémaud B. and Delande D.: Europhys. Lett. **40**, 363 (1997).
4. Richter K. and Wintgen D.: Phys. Rev. Lett. **65**, 1965 (1990).
5. Tannor G., Richter K., and Rost J.M.: Rev. Mod. Phys. **72**, 497 (2000).
6. Rost J.M., Schulz K., Domke M., and Kaindl G.: J. Phys. B **30**, 4663 (1997); Püttner R., Grémaud B., Delande D., Domke M., Martins M., Schlachter A.S., and Kaindl G.: Phys. Rev. Lett. **86**, 3747 (2001).
7. Giannoni M.J., Voros A., and Zinn-Justin J. (eds.): "Chaos and Quantum Physics", North-Holland, Amsterdam 1991.
8. Weber T. et al.: Nature **405**, 658 (2000).
9. Moshammer R. et al.: Phys. Rev. A **65**, 35401 (2002).

10. Taylor K., Parker J.S., Meharg K.J., and Dundas D.: Eur. Phys. J. D **26**, 67 (2003).
11. Lambropoulos P., Maragakis P., and Zhang J.: Phys. Rep. **305**, 203 (1998).
12. Scrinzi A. and Piraux B.: Phys. Rev. A **56**, R13 (1997).
13. Purvis J., Dörr M., Terao-Dunseth M., Joachain C.J., Burke P.G., and Noble C.J.: Phys. Rev. Lett. **71**, 3943 (1993).
14. Shirley J.H.: Phys. Rev. **138**, B979 (1965).
15. Ho Y.K.: Phys. Rep. **99**, 1 (1983).
16. Krug A. and Buchleitner A.: Phys. Rev. A **66**, 53416 (2002).
17. Madroñero J.: *Spectral properties of planar helium under periodic driving*, Dissertation, Ludwig-Maximilians-Universität München, submitted (2004).
18. Sacha K. and Eckhardt B.: Phys. Rev. A **63**, 043414 (2001).
19. Zrost K., Rudenko A., de Jesus V.L.B., Ergler T., Schröter C.D., Moshammer R., and Ullrich J.: oral presentation at *Energiereiche Atomare Stöße*, 8-13 February 2004, Riezlern.
20. Stébé B. and Ainane A.: Superlattices and Microstruct. **5** 545 (1989).
21. Nazmitdinov R.G., Simonović N.S., and Rost J.M.: Phys. Rev. B **65**, 155307 (2002).
22. Hilico L., Grémaud B., Jonckheere T., Billy N., and Delande D.: Phys. Rev. A **66**, 22101 (2002).
23. Karypis G. and Kumar V.: J. Parall. Distrib. Comp. **48**(1), 96 (1998).
24. http://www.lrz-muenchen.de/services/compute/hlrb/hardware-en/
25. http://www.rzg.mpg.de/computing/IBM_P/
26. Krug A. and Buchleitner A.: in *High Performance Computing in Science and Engineering. Munich 2002*, Transactions of the First Joint HLRB and KONWIHR Result and Reviewing Workshop, 10-11 October 2002, Munich.
27. Eichmann U., Lange V., and Sandner W.: Phys. Rev. Lett. **64**, 274 (1990).
28. Schlagheck P. and Buchleitner A.: Eur. Phys. J. D **22**, 401 (2003).
29. Lappas D.G., Sanpera A., Watson J.B., Burnett K., Knight P.L., Grobe R., and Eberly J.H.: J. Phys. B **29**, L619 (1996); Lein M., Gross E.K.U., and Engel V.: Phys. Rev. Lett. **85**, 4707 (2000).
30. Richter K., Briggs J.S., Wintgen D., and Solovev E.A.: J. Phys. B **25**, 3929 (1992).
31. Tomsovic S. and Ullmo D.: Phys. Rev. E **50**, 145 (1994); Zakrzewski J., Delande D., and Buchleitner A.: Phys. Rev. Lett. **75**, 4015 (1995).
32. Assion A., Naumert T., Bergt M., Brixner T., Kiefer B., Seyfried V., Strehle M., and Gerber G.: Science **282**, 919 (1998); Weinacht T.C., Ahn J., Bucksbaum P.H.: Nature **397**, 233 (1999); Arbo D.G., Reinhold C.O., and Burgdörfer J.: Phys. Rev. A **69**, 23409 (2004).
33. Hanson L.G. and Lambropoulos P.: Phys. Rev. Lett. **77**, 2186 (1996).
34. Buchleitner A.: *Atomes de Rydberg en champ micro-onde: regularité et chaos*, thèse de doctorat, Université Pierre et Marie Curie, Paris 1993.
35. Delande D. and Buchleitner A.: Adv. At. Mol. Opt. Phys. **34**, 85 (1994).
36. Białynicki-Birula I., Kalinski M., and Eberly J.H.: Phys. Rev. Lett. **73**, 1777 (1994).
37. Brunello A.F., Uzer T., and Farelly D.: Phys. Rev. Lett. **76**, 2874 (1996).
38. Buchleitner A., Delande D., and Zakrzewski J.: Phys. Rep. **368**, 409 (2002).
39. Maeda H. and Gallagher T.F.: Phys. Rev. Lett., in print (2004).
40. Schlagheck P. and Buchleitner A.: Physica D **131**, 110 (1999).

41. Graham R.: Comm. At. Mol. Phys. **25**, 219 (1991).
42. Raman C., Weinacht T.C., and Bucksbaum P.H. : Phys. Rev. A **55**, R3995 (1997).